Journal of Thermal Analysis and Calorimetry, Vol. 88 (2007) 1, 171–176

TiO_2-BASED NANOPOWDERS OBTAINED FROM DIFFERENT Ti-ALKOXIDES

M. Crişan[1*], *Ana Brăileanu*[1], *M. Răileanu*[1], *D. Crişan*[1], *V. S. Teodorescu*[2], *R. Bîrjega*[3], *V. E. Marinescu*[4], *J. Madarász*[5] *and G. Pokol*[5]

[1]Roumanian Academy, Institute of Physical Chemistry Ilie Murgulescu, 202 Splaiul Independenţei, 060021 Bucharest, Roumania
[2]National Institute for Physics of Materials, P.O. Box MG 07, Bucharest, Măgurele, Roumania
[3]National Institute for Lasers, Plasma and Radiation Physics, PO Box MG-36, Bucharest, Roumania
[4]INCDIE ICPE-CA, 313 Spl. Unirii, 030138 Bucharest, Roumania
[5]Budapest University of Technology and Economics, Institute of General and Analytical Chemistry, Szt. Gellért tér 4 1521 Budapest, Hungary

Pure TiO_2 and S-doped TiO_2 sol–gel nanopowders were prepared by controlled hydrolysis-condensation of titanium alkoxides. The influence of different Ti-alkoxides (tetraethyl-, tetraisopropyl- and tetrabutyl-orthotitanate) used in obtaining TiO_2 porous materials in similar conditions (water/alkoxide ratio, solvent/alkoxide ratio, pH and temperature of reaction) has been investigated. The relationship between the synthesis conditions and the properties of titania nanosized powders, such as thermal stability, phase composition, crystallinity, morphology and size of particles, BET surface area and the influence of dopant was investigated. The nature of the alkyl group strongly influences the main characteristics of the obtained oxide powders, fact which is pointed out by thermal analysis, X-ray diffraction, TEM and BET surface area measurements.

Keywords: *S-doped TiO_2, sol–gel method, thermal analysis, TiO_2 nanopowders*

Introduction

Sol–gel processing is one of the most common methods to produce nanoparticles with controlled size and composition for a wide range of applications. Starting from molecular precursors such as metal alkoxides, an oxide network is obtained via inorganic polymerization reactions [1]. Low temperature solution processing with high purity, the facility of precise control of complex chemical composition and physical structure, control of pore structure and pore-wall chemistry, ready preparation of thin films and coatings or nanocrystalline powders, versatile inorganic/organic composite preparation and availability of good optical quality materials are all valuable attributes for development of new functional materials [2].

There is increasing interest in development of chemically stable materials with porous texture in the fields of separation and catalysts, owing to their high specific areas and pore volumes, as well as their narrow pore size distributions. Titania has been widely used as a catalyst in organic reactions such as selective oxidation and photocatalytic reactions such as alcohol dehydration, photo-Kolbe oxidation of organic acids, oxidation of aromatic compounds, degradation of paint pigments and nitrogen oxides reduction [3].

In order to obtain powders, sol–gel refers to processing in a liquid medium to obtain a solid matter which does not precipitate. The first occurrence of solid particles in solution (primary particles) can be described as a succession of chemical reactions, from an initial chemical compound of a cation (Ti), called the precursor. In the presence of water, the precursor undertakes the following succession of transformations: hydrolysis→polymerization→nucleation→growth [4]. When alkoxides are used, the precursor concentration and the water concentration for hydrolysis can be controlled by dissolution in a solvent which is often the parent alcohol of the precursor.

Hydrolysis of alkoxides is the most common method of producing TiO_2 nanopowders. It is recognized that process parameters have a major influence on the properties of the sol–gel products. These factors include the alkoxy groups of alkoxides, the concentration of reactants, the pH of solution, the temperature of hydrolysis, the nature of catalyst and the influence of dopants. In our previous papers [5–7] a systematic study of the influence of the type of Ti-alkoxide on the preparation and properties of TiO_2 coatings for ceramic membranes or films with optical properties has been presented.

Nevertheless, TiO_2 becomes active only under ultraviolet (UV) light, of which energy is greater than the band gap of TiO_2 (~3.0 eV) [8]. In order to improve the photoreactivity of TiO_2 and to extend its absorption edge into the visible-light region, the new lit-

* Author for correspondence: abrail@icf.ro

1388–6150/$20.00

Akadémiai Kiadó, Budapest, Hungary
Springer, Dordrecht, The Netherlands

erature data pointed out S-doped TiO_2 particles [9–16].

There are many papers dealing with the sol–gel preparation of TiO_2 anatase with tailored morphological features and some of them review the thermal behaviour of the TiO_2 gels complemented by other investigations [17–20]. Only few literature data concerning the thermal behaviour of S-doped TiO_2 can be mentioned [21].

In the present work pure TiO_2 and S-doped TiO_2 sol–gel nanopowders were prepared by controlled hydrolysis-condensation of titanium alkoxides. The influence of different Ti-alkoxides (tetraethyl-, tetraisopropyl- and tetrabutyl-orthotitanate) used in obtaining TiO_2 nanopowders in similar conditions (water/alkoxide ratio, solvent/alkoxide ratio, pH and temperature of reaction) has been investigated. The relationship between the synthesis conditions and the properties of titania nanosized powders, such as thermal stability, phase composition, crystallinity, morphology and size of particles, BET surface area and the influence of dopant were investigated.

Experimental

Three different types of titanium alkoxides have been used in order to obtain TiO_2 based oxide materials:

- tetraethylorthotitanate (Merck), $Ti(OC_2H_5)_4$ for the sample 1-TiO_2;
- tetraisopropylorthotitanate (Merck), $Ti(O\text{-}iC_3H_7)_4$ for the sample 2-TiO_2;
- tetrabutylorthotitanate (Fluka), $Ti(O\text{-}C_4H_9)_4$ for the sample 3-TiO_2.

As solvents and media of reaction the corresponding parent alcohols were used: absolute ethanol (Riedel de Haën) for the sample 1-TiO_2, 2-propanol (Fluka) for the sample 2-TiO_2 and normal butanol (J. T. Baker) for the sample 3-TiO_2. The hydrolysis of titanium alkoxides took place with a water excess in uncatalysed reaction mixture. In order to point out exclusively the role of alkoxide type on the structural, textural and morphological properties of TiO_2 powders, all the other reaction parameters were similar: e.g a water/alkoxide molar ratio of 5, a solvent/alkoxide molar ratio of 85, a pH of 4 and a temperature of reaction of 25°C. The reaction time varied between 1–6 h, depending on the type of alkoxide precursor.

The samples 4-S-TiO_2, 5-S-TiO_2, 6-S-TiO_2 are obtained in similar conditions with the first ones, but were doped with S-5% mass related to TiO_2 content. As sulfur source, thiourea Alfa Aesar (H_2NCSNH_2), dissolved in the corresponding alcohol, was used. The obtained sols were concentrated and dried at 80°C and the powders resulted were subjected to thermal analysis measurements in order to establish the thermal schedule for further investigations. Thus, for structural and morphological studies, the powders were thermally treated up to 300°C with a heating rate of 1°C min^{-1} and kept for 1 h at this temperature, in order to remove the organic matter. To study the influence of the crystallization process on the shape and size of particles, the samples were also annealed at 400°C, with the same heating rate and plateau.

The TiO_2 and S-TiO_2 nanopowders were characterized by:

- Thermal analysis, on dried samples performed using a STA 409 PC Luxx simultaneous DSC and TG/DTG equipment (Netzsch), up to 700°C in static air atmosphere, with a heating rate of 10 K min^{-1}. 14–16 mg of powders were analysed using a 85 μL alumina crucible.
- X-ray diffraction, using a computer controlled DRON DART UM-2 diffractometer equipped with a CuK_α source and a graphite monochromator in the diffracted beam (scanning technique was applied with a step width of 0.05° and an acquisition time on each step of 2 s, ranging from 2θ=15–60°). The mean crystallite sizes were determined from the corrected FWHM (full width at half maximum) applying the Debye–Scherrer formula.
- BET surface area measurements with Quantachrome Instruments-Nova 1000;
- TEM with Jeol 200CX and HRTEM with Topcon 002B equipments.

Results and discussion

Thermal analysis

Thermal behaviour of the un-doped samples (1–3-TiO_2) is presented in Figs 1a–c. All DSC curves of the mentioned samples show a broad endothermic effect at ~100°C due to adsorbed water and alcohol removal and an exothermic effect at ~250°C, more pronounced for the sample 2 and even more for the sample 3. This effect is associated with mass losses on TG curves (5.61 and 6.12%) and DTG maxima at 221.6 and 248.5°C for samples 2 and 3, respectively, which are attributed to the thermooxidative degradation of the organic matter. Only DSC curves of the samples 1 and 2-TiO_2 present very sharp crystallization effects of TiO_2-anatase at 403.5 and 412.4°C, respectively. For the sample 3 one can observe a less sharp exothermic effect at around 500°C, correlated with a mass loss on the TG curve (5.63%), probably due to the burning out of the organic residues. This fact is correlated with the length of the alkyl chain of the Ti alkoxide precursor.

DSC/TG/DTG curves of S-doped samples (4–6-TiO_2), presenting complex thermal effects due

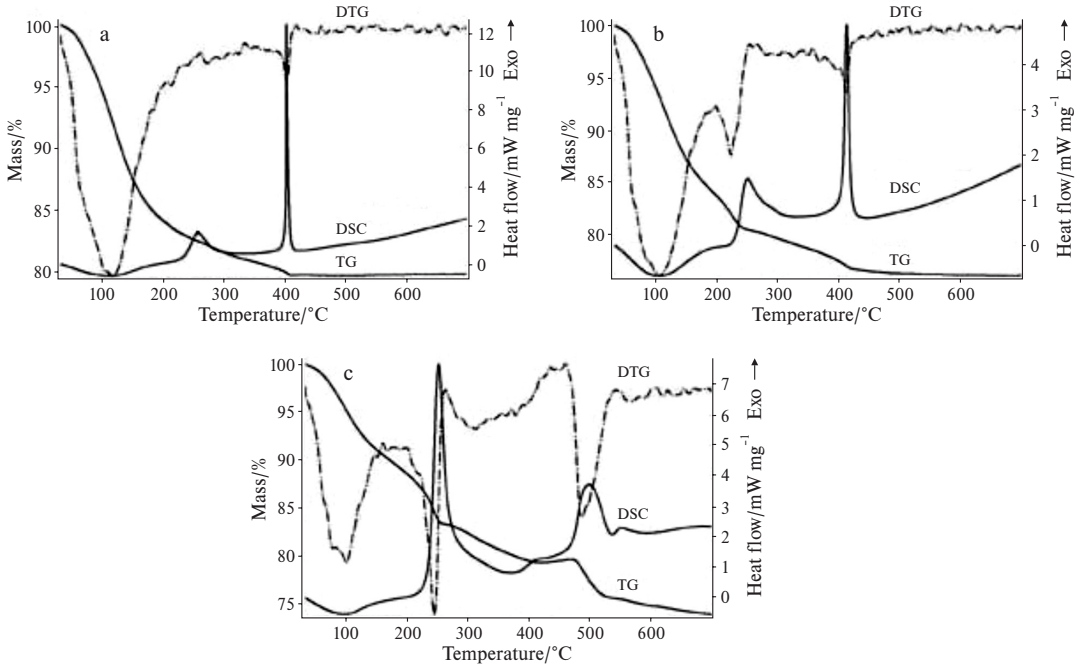

Fig 1 Thermal behaviour in static air atmosphere of the un-doped samples: a – 1-TiO_2; b – 2- TiO_2; c – 3- TiO_2

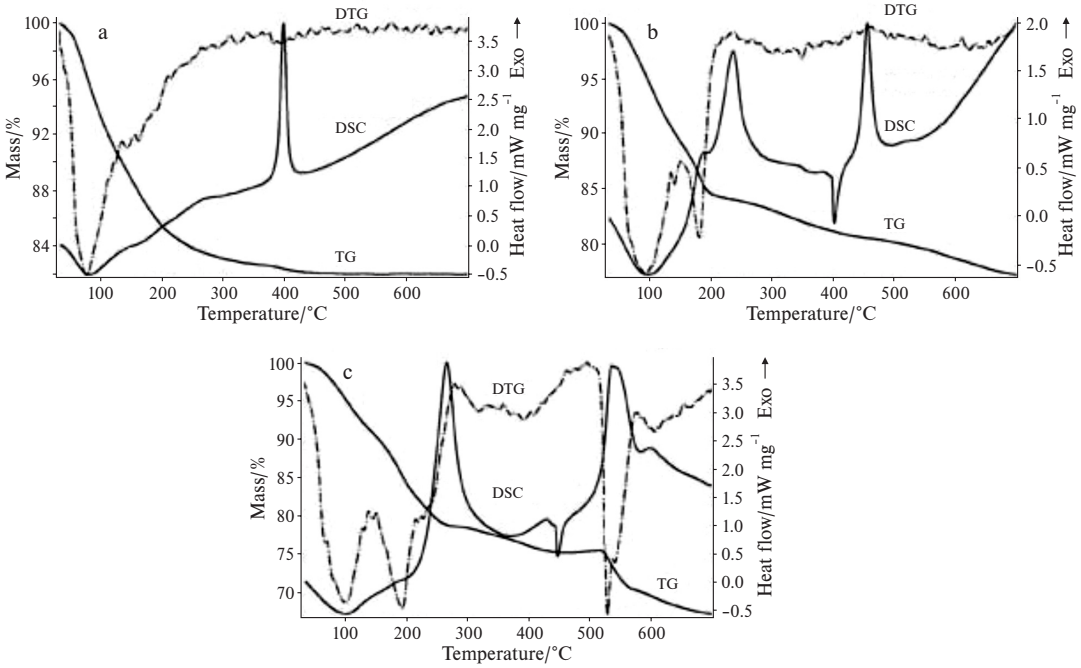

Fig. 2 Thermal behaviour in static air atmosphere of the S-doped samples: a – 4-S-TiO_2; b – 5-S-TiO_2; c – 6-S-TiO_2

to the influence of the thiourea (S-source), are shown in Figs 2a–c. Thermal decomposition of the compounds containing thiourea is usually quite complex [22, 23].

The DSC curves of the S-doped TiO_2 samples, as well as those of the un-doped TiO_2 ones, show a broad endothermic effect at about 100°C due to adsorbed water and alcohol removal, correlated with mass losses on TG curves. Further mass losses associated with DTG maxima, more pronounced for the samples 5-S-TiO_2 and 6-S-TiO_2 were noticed at 179 and 189°C, respectively. These ones are probably due to the decomposition of residues from thiourea that may be expected at around the melting point of pure thiourea, which melts at 180°C with decomposition [24]. Exothermic effects at ~264, 235 and 263°C, respectively, much more pronounced for 5-S-TiO_2 and 6-S-TiO_2 samples are present on DSC curves, attrib-

uted to the thermooxidative degradation of the organic matter. With the temperature increase, only the DSC curve of the sample 4 presents a very sharp crystallization effect of TiO_2-anatase at ~398°C. One can mention, for the samples 5 and 6, the presence on the DSC curve, at 401 and 447.5°C, respectively, of a supplementary endothermic effect, which is not associated with mass loss on TG curve. For the sample 5, a pronounced exothermic effect is noticed at 455°C, related to the anatase crystallization. For the sample 6, at 535°C, like for the sample 3, at 500°C, a less sharp but quite intense exothermic effect, associated with a mass loss on the TG curve, can be observed (8.18% for sample 6 and 5.63% for sample 3).

As a conclusion of the thermal behaviour study, the influence of the Ti-alkoxide type on the crystallization temperature of TiO_2 anatase was evidenced. The increase of the alkyl chain length of the Ti-alkoxide leads to the increase of the crystallization temperature of TiO_2 anatase phase. To get a better understanding of the gradual decomposition processes leading to anatase formation, an additional evolved gas analytical study is also planned on the samples prepared.

X-ray diffraction and BET measurements

Phase composition established by XRD measurements and the BET surface area results are presented in Tables 1 and 2.

TiO_2 powders have a pronounced crystallization tendency with temperature, especially in the case of sample 1, prepared starting with titanium ethoxide precursor. As a consequence, the BET surface area decreases with the temperature increase *vs.* the crystalline phase formed at different temperatures.

In order to establish the manner in which S influences the structural properties of the powders, the samples were thermally treated at the same temperature, 400°C/1 h. A single phase, anatase, has been detected. Sulfur decreases the degree of crystallinity and inhibits the rate of growing of TiO_2 nanocrystals. XRD patterns of the un-doped and S-doped samples, thermally treated at 400°C/1 h, are presented in Fig. 3.

TEM analysis

The statistical processing of the TEM images evidenced the presence in all the samples of spheroidal TiO_2 nanocrystallites, joined in aggregates with sizes between 300 and 800 nm. For the samples 1-TiO_2 and 4-S-TiO_2, prepared starting with titanium ethoxide precursor, these aggregates have spherical morphology.

HRTEM images for sample 1-TiO_2 dried (Fig. 4a) and thermally treated at 400°C/1 h (Fig. 4b) and for sample 2-TiO_2 thermally treated at 400°C/1 h (Fig. 5) are representative.

Table 1 Structural and textural properties of the un-doped samples *vs.* thermal processing

Sample	Temperature/ °C	Phase composition	Degree of crystallinity/%*	D_{101}/ Å	BET surface area/ $m^2\ g^{-1}$
1-TiO_2	80	amorphous			251
	300	anatase weak crystallized			130
	400	anatase	100	168	94
	1000	rutile			1
2-TiO_2	80	amorphous			344
	300	anatase weak crystallized			141
	400	anatase	97	133	115
	1000	rutile			1
3-TiO_2	80	amorphous			188
	300	amorphous			111
	400	anatase	65	172	80
	1000	rutile			1

*the degree of crystallinity was estimated using sample 1 as internal reference sample from the sum of integrated intensities (area under deconvoluted peaks) of the (101), (103), (004), (112), (200), (105) and (211) reflections

Table 2 Structural properties of the S-doped samples, thermally treated at 400°C/1 h

Sample	Temperature/°C	Phase composition	Degree of crystallinity/%	D_{101}/Å
4-S-TiO_2	400	anatase	98	147
5-S-TiO_2	400	anatase	73	113
6-S-TiO_2	400	anatase	56	158

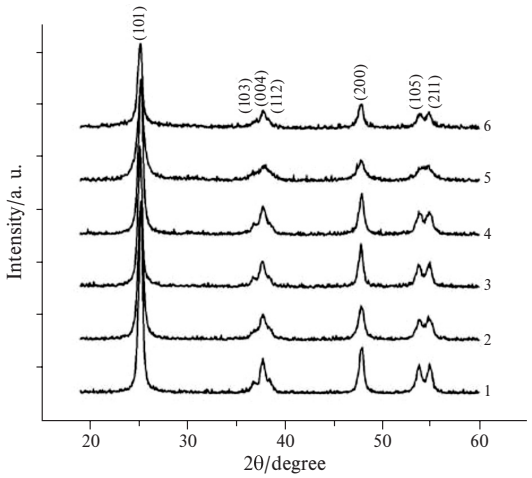

Fig. 3 XRD patterns of the un-doped and S-doped samples, thermally treated at 400°C/1 h

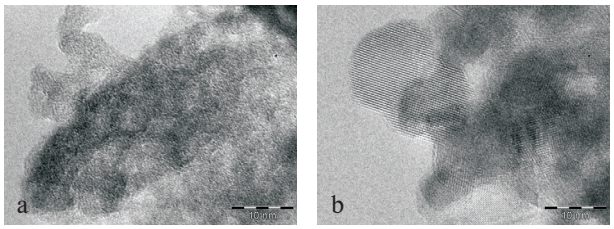

Fig. 4 HRTEM images of the sample 1-TiO_2: a – dried; b – thermally treated at 400°C/1 h

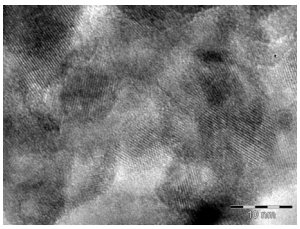

Fig. 5 HRTEM images of the sample 2-TiO_2 thermally treated at 400°C/1 h

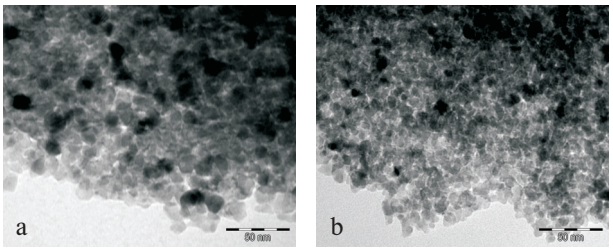

Fig. 6 TEM images of the samples a – 3-TiO_2 and b – 6-S-TiO_2, both thermally treated at 400°C/1 h

Conventional TEM images for samples 3-TiO_2 and 6-S-TiO_2, presented in Fig. 6, show the difference in size for the un-doped and S-doped samples. Corresponding measured size distributions are exposed in Fig. 7. The mean size decreases from 12.7 to 8.9 nm in the presence of sulfur.

For the samples 5-S-TiO_2 and 6-S-TiO_2, the amorphous phase vanishes, leading to more compact aggregates. The role of sulfur is to reduce the nanocrystallite size and also to densify the nanocrystallite aggregates.

Differences in reactivity related to differences in structure of the molecular precursors have been observed for titanium alkoxides [25], so that especially, the morphology of TiO_2 powders strongly depends on the nature of the alkoxy group. Titanium alkoxides with primary alkoxy groups are trimeric species with a pentacoordinated metal atom while those with secondary or tertiary alkoxy groups are monomers with titanium in a tetrahedral environment. These different structures lead to different behaviour towards hydrolysis and condensation and have a great influence on the morphology of TiO_2 powders. The fourfold coordinated monomeric species of $Ti(O\text{-}iC_3H_7)_4$ are more reactive. Hydrolysis and condensation proceed simultaneously leading to shapeless nanoparticles with an average diameter of 11.4 nm joined in aggregates with sizes of 200 to 400 nm, in agreement with literature data [25, 26]. Hydrolysis of $Ti(OC_2H_5)_4$ in the

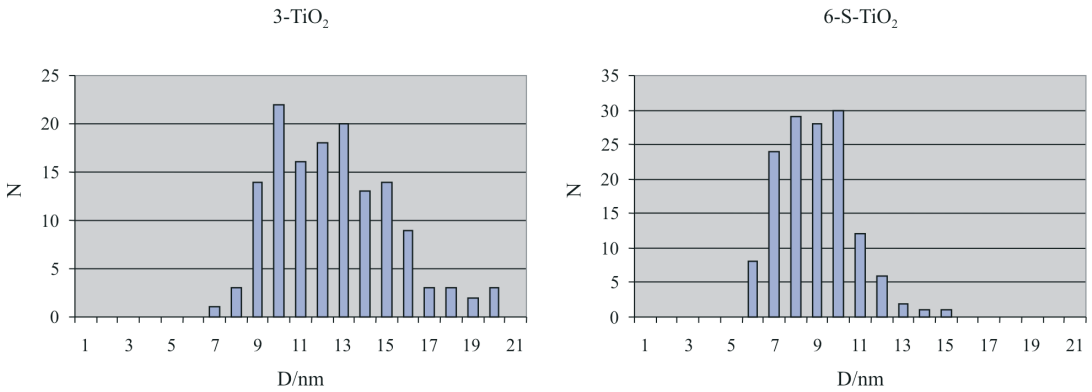

Fig. 7 Size distributions from the statistical processing of the TEM images for the a – samples 3-TiO_2 and b – 6-S-TiO_2

same conditions leads to monodispersed TiO_2 particles, with a narrow size distribution and an average diameter of 11.7 nm. In this case the nanocrystallite aggregates are generally spherical with sizes of 300 to 800 nm.

Also, hydrolysis of titanium *n*-alkoxides becomes slower when the size of the alkyl group increases [1]. The positive partial charge of Ti decreases with the length of the alkyl chain [δ(Ti)=+0.63 for R=C_2H_5 and +0.61 for R=*n*-C_4H_9] [1], which determines the decrease of the sensitivity of the butoxide towards hydrolysis. Experimental results are often explained in terms of steric hindrance as well. It has been shown that, for isomeric titanium butoxides, the hydrolysis rate decreases in the order tertiary>secondary>normal. Thus, the powder obtained from Ti-butoxide has the greatest size of particle (mean size diameter=12.7 nm for sample 3-TiO_2), which correlates with the smallest values of the surface area (Table 1).

Conclusions

Pure TiO_2 and S-doped TiO_2 sol–gel nanopowders were prepared by controlled hydrolysis-condensation of titanium alkoxides. The influence of different Ti-alkoxides (tetraethyl-, tetraisopropyl- and tetrabutyl-orthotitanate) used in obtaining of TiO_2-based nanopowders in similar conditions (water/alkoxide ratio, solvent/alkoxide ratio, pH and temperature of reaction) has been investigated.

The main characteristics of oxide powders (particle size, surface area, morphology and crystalline phases) obtained by hydrolysis and condensation of titanium alkoxides depend in a great extent on the nature of the alkyl group. Thermal analysis, X-ray diffraction, TEM and BET surface area measurements pointed out this fact. The increase of the alkyl chain length of the Ti-alkoxide leads to the increase of the crystallization temperature of TiO_2 anatase phase.

Sulfur decreases the degree of crystallinity and inhibits the rate of growing of TiO_2 nanocrystals, leading to more compact nanocrystallite aggregates.

Acknowledgements

This work was supported partially by the National Research Program CEEX No. 6113/2005-2008 and CEEX No. 642/2005-2008.

References

1 J. Livage, M. Henry and C. Sanchez, Prog. Solid State Chem., 18 (1988) 259.
2 J. D. Wright and N. A. J. M. Sommerdijk, Sol-Gel Materials Chemistry and Applications, Gordon and Breach Science Publishers, 2001, p. 109.
3 J. Yu, J. C. Yu, W. Ho and Z. Jiang, New J. Chem., 26 (2002) 607.
4 A. C. Pierre, Ceram. Bull., 70 (1991) 1281.
5 M. Crişan, M. Zaharescu, D. Crişan and L. Simionescu, Adv. Sci.Technol., B3 (Ceramics Charting the Future), P. Vincenzini, Ed., Faenza, Italy 1995, p. 2805.
6 M. Crişan, M. Zaharescu, L. Simionescu and D. Crişan, Proceedings of Euromembrane'95, W. R. Bowen, R. W. Field and J. A. Howell, Eds, University of Bath, 1 (1995) I-341.
7 M. Zaharescu, M. Crişan, D. Crişan, M. Gartner and F. Moise, Rev. Roum. Chim., 40 (1995) 993.
8 J. Pascual, J. Camassel and H. Mathieu, Phys. Rev. Lett., 39 (1977) 1490.
9 S. Yamazaki, N. Fujinaga and K. Araki, Appl. Catal. A: General, 210 (2001) 97
10 T. Umebayashi, T. Yamaki, H. Itoh and K. Asai, Appl. Phys. Lett., 81 (2002) 454.
11 T. Ohno, T. Mitsui and M. Matsumura, Chem. Lett., 32 (2003) 364.
12 T. Tachikawa, S. Toja, K. Kawai, M. Endo, M. Fujitsuka, T. Ohno, K. Nishijima, Z. Miyamoto and T. Majima, J. Phys. Chem., 108 (2004) 19299.
13 T. Ohno, M. Akiyoshi, T. Umebayashi, K. Asai, T. Mitsui and M. Matsumura, Appl. Catal. A: General, 265 (2004) 115.
14 Q. Yang, C. Xie, Z. Xu, Z. Gao and Y. Du, J. Phys. Chem. B., 109 (2005) 5554.
15 R. Bacsa, J. Kiwi, T. Ohno, P. Albers and V. Nadtochenko, J. Phys. Chem. B., 109 (2005) 5994.
16 H. Wang and J. P. Lewis, J. Phys: Condens. Matter, 18 (2006) 421.
17 R. Campostrini, M. Ischia and L. Palmisano, J. Therm. Anal. Cal., 71 (2003) 997.
18 R. Campostrini, M. Ischia and L. Palmisano, J. Therm. Anal. Cal., 71 (2003) 1011.
19 R. Campostrini, M. Ischia and L. Palmisano, J. Therm. Anal. Cal., 75 (2004) 13.
20 R. Campostrini, M. Ischia and L. Palmisano, J. Therm. Anal. Cal., 75 (2004) 25.
21 H. Sun, Y. Bai, Y. Cheng, W. Jin and N. Xu, Ind. Eng. Chem. Res., 45 (2006) 4971.
22 M. Krunks, J. Madarász, L. Hiltunen, R. Mannonen, E. Mellikov and L. Niinistö, Acta Chem. Scand., 51 (1997) 294.
23 J. Madarász, P. Bombicz, M. Okuya and S. Kaneko, Solid State Ionics, 141–142 (2001) 439.
24 J. Madarász and G. Pokol, J. Therm. Anal. Cal., 2007, in press (ESTAC 9 issue, Ms. No. 8058, revised).
25 C. Sanchez and J. Livage, New J. Chem., 14 (1990) 513.
26 E. A. Barringer and H. K. Bowen, J. Am. Ceram. Soc., 65 (1982) C-199.

DOI: 10.1007/s10973-006-8125-x